Directly mapping whispering gallery modes in a microsphere through modal coupling and directional emission

Chunhua Dong (董春华)[1], Yunfeng Xiao (肖云峰)[1], Yong Yang (杨 勇)[1], Zhengfu Han (韩正甫)[1], Guangcan Guo (郭光灿)[1], and Lan Yang[2]

[1]*Key Laboratory of Quantum Information, University of Science and Technology of China, Hefei 230026*

[2]*Department of Applied Physics, California Institute of Technology, Pasadena, California 91125, USA*

Received October 9, 2007

We fabricate slightly deformed fused-silica microspheres in which whispering gallery modes possess remarkably directional escape emission from the microsphere boundary. With efficient free-space excitation and collection, the lateral spatial distribution of whispering gallery modes with different azimuthal mode numbers, m, is directly observed through modal coupling and directional emission. Excellent agreement with theory is obtained.

OCIS codes: 140.3410, 230.5750, 350.3950.

Whispering gallery (WG) modes in spherical or other symmetrical systems have long been considered as candidates for a large variety of optical applications that require high quality-factor (Q) and small mode-volume (V) resonators, such as ultra-low-threshold lasers, sensors, optoelectronic devices[1−3], atom-field coherent interactions[4−7], and quantum information processing[8−11]. WG modes in microspheres are characterized completely by the TE or TM polarization and three mode numbers: radial (q), orbital (l), and azimuthal (m). In particular, m can take integer values $-l, -l+1, \cdots, l-1, l$, and the angular (or lateral) distributions of the WG modes are approximately given by spherical harmonics functions $Y_{lm}(\theta, \varphi)$.

An understanding of the maxima of local field and their spatial distribution is of importance in many applications ranging from cavity quantum electrodynamics (QED) to biosensing since it directly affects coupling strength of a local polarizability at the surface of the resonator to the WG modes. In this regard, mapping of the intensity distribution of the WG modes has been performed in several ways including collection of very weak scattering by a precisely controlled near-field probe[12,13] and imaging of upconverted photoluminescence from an Er^{3+}-doped microsphere[14]. In this paper, we report direct mapping of WG modes in a deformed microsphere through the modal coupling[15,16] and directional emission mechanisms[17]. Imaging in the experiment relies upon coupling of clockwise (CW) and counterclockwise (CCW) modes within the WG. In the ideal case of a perfectly smooth sphere, each WG mode possesses a natural two-fold degeneracy. This degeneracy is, however, broken when a part of the mode energy (e.g. CW mode) is coupled into the opposite-propagation-direction (e.g. CCW mode)[18]. Using this modal coupling, the CCW mode emission can be observed by exciting the CW mode, providing for a relatively low background noise signal (i.e. free of the excitation beam). Coupling to the WG normally relies upon proper phase matching of the excitation wave to the desired WG mode. This can be accomplished using prisms, angle polished fiber or tapered silica fibers, which provide the highest coupling efficiency[19]. However, in the present case, where modal imaging is desired, it is useful to couple directly to free space modes. Asymmetric resonant cavities (ARCs) are chosen because their broken, rotational symmetry leads to directional emission to free space from the WG[20−23]. Strong directional emission[24] has been observed in deformed microspheres by melting two similar-size spheres, and normal mode splitting was observed in this kind of deformed microsphere cavity QED system[25]. This opens the door to employ strong-coupling physics in ARCs.

In our experiment, we fabricated a microsphere with a relatively large spherical eccentricity, which induces a large energy splitting among the different azimuthal mode numbers m. First, a filament of fiber was prepared from a standard optical fiber using a CO_2 laser heating process. A microsphere with a desired diameter was achieved by reheating the fiber tip[26]. Then the microsphere was stretched along the polar direction by slightly penetrating a sharp fiber tip with a diameter of about 5 μm into the bottom of the soft molten sphere. Subsequently the tip was gently pulled back and then broken at a position close to the microsphere by a strong irradiation power. The bottom of the microsphere was further gently heated by the CO_2 laser until the residual fiber tip melted into the sphere due to the surface tension. A spheroid whose eccentricity could be modulated by controlling the pulling distance was formed. Very importantly, this pulling procedure also induced a small deformation in the equatorial plane of the sphere due to misalignment between the tip and the polar axis of the sphere. In particular, this "asymmetry" in equatorial plane is critical to the coupling strategy employed in this work. The equatorial plane of the sphere approximatively exhibits a combination of a half-circle and a half-ellipse, and the deformation, $(R_{\max} - R_{\min})/(R_{\max} + R_{\min})$ (where $R_{\max}$,

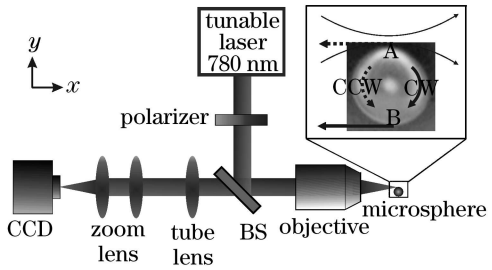

Fig. 1. Experimental setup. A tunable laser beam (TE mode, ~ 0.1 mW, $764-781$ nm) was focused into a waist smaller than 10 μm using an objective (20×). Emission from the microsphere was collected using the same lens and directly monitored by a high resolution and high sensitivity charge coupled device (CCD) camera. BS: beam splitter.

$R_{\min}$ are the maximal and minimal radii of the equatorial plane), is about 1.3%. Q factors maintain up to 10^7 in despite of this deformation. The dissipation mechanisms, such as intrinsic radiation, scattering on residual surface inhomogeneities, and material absorption can be regarded as a background loss, and the dominating dissipation mechanism is not the refractive loss, but the tunneling emission at the point A with the highest curvature, as shown in Fig. 1.

To observe the spatial modes of this structure, a tunable laser was focused near the edge of the sphere, in the vicinity of point A. The CW modes in the microsphere were excited. In our measuremnt, we always observed a bright emission in the direction B (Fig. 1), which can be understood as due to the coupling to low-Q modes. These modes have the CW sense of circulation in Fig. 1. At the same time, as shown in Fig. 2(a), there is little or no backscatter coupling into the CCW mode whose emission would appear on the right side of the image. All the measurements should be taken care, so as to create only "grazing" incident coupling between the excitation beam and the microsphere. The realization of such weak coupling is evidenced by the fact that no scattering is observed on the right side of the sphere in Fig. 2(a).

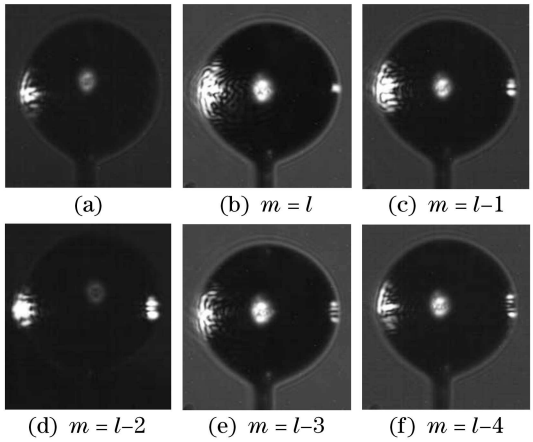

Fig. 2. Typical emission patterns of microsphere (input power, 0.1 mW). Image (a) describes the general case when only low-Q modes are excited while (b)—(f) show cases when high-Q modes are excited and the excitation wavelengths are 766.55, 766.80, 767.05, 767.31, and 767.53 nm, respectively. The right (left) edge in each image corresponds to the point A (B) in Fig. 1.

On the other hand, at some specific excitation wavelengths, high-Q CW modes were effectively excited due to the frequency matching. These CW modes have a dramatically improved coupling to the corresponding CCW modes because they have a long photon lifetime. At point A (right side of sphere in Figs. 2(b)—(f)), where the highest curvature results in the largest evanescent loss, directional emission was observed. As this emission direction only couples power that is present in the CCW modes, it has very low background and enables the direct observation of the spatial mode structure of the CCW modes. As a result, the modal coupling plays a significant role in the observation of the directionally emitted CCW modes at the point A. Figures 2(b)—(f) show the observed patterns, corresponding to $|m| = l$, $l-1$, $l-2$, $l-3$, $l-4$, respectively. These modes were specifically addressed by varying the excitation wavelength. It is estimated that the orbital number is $l = 238$, corresponding to a diameter of 42 μm and an approximate excitation wavelength of 767 nm. The mode spacing depends on the size and the eccentricity of the microsphere. The spacing is about 0.25 nm in our measured sphere, which corresponds to an 8% sphere eccentricity. The departure from spherical symmetry was also studied by considering the supporting structure and anisotropy of the material[27,28].

To quantitatively characterize the lateral intensity distributions of the WG modes in the deformed microsphere, we directly read out the brightness of the images in Figs. 2(b)—(f). As shown in Fig. 3, we plotted the patterns after normalization. The solid lines describe the measured intensity distribution while the dashed lines give the theoretically expected intensity distributions for these modes. It shows that the measured curves are coincident with the theoretical prediction.

Finally we briefly discuss how the modal coupling and the directional emission mechanisms in a deformed microsphere play central roles in our experiments. For a

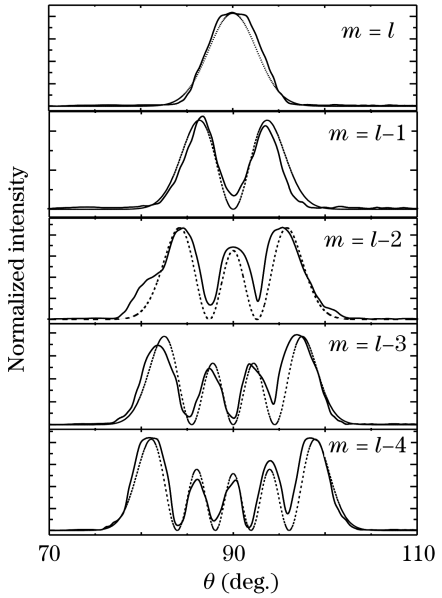

Fig. 3. Experimental (solid lines) and theoretical (dashed lines) normalized lateral intensity distributions of WG modes for different azimuthal numbers m corresponding to the same orbital number l. θ is the polar angle.

deformed microsphere cavity described above, we focus on a pair of degenerate CW and CCW modes with frequency ω. There are two decay paths: 1) directional decay with associated loss coefficients $\kappa_1^{\rm cw}$ and $\kappa_1^{\rm ccw}$, and 2) isotropic decay, including material absorption, surface scattering, surface contaminant etc., described by $\kappa_0^{\rm cw}$ and $\kappa_0^{\rm ccw}$ respectively. To facilitate the discussion, we suppose that the CW and CCW modes have different propagation directions but the same decay characteristics denoted by $\kappa_0^{\rm cw} = \kappa_0^{\rm ccw} = \kappa_0$, $\kappa_1^{\rm cw} = \kappa_1^{\rm ccw} = \kappa_1$, $\kappa^{\rm cw(ccw)} = \kappa_0^{\rm cw(ccw)} + \kappa_1^{\rm cw(ccw)}$. We also suppose there is no input to the CCW mode. According to the equations of motion[10,11] or coupled mode theory[6,8], the reflection from CCW to CW modes can be obtained as $R = \left|\kappa_1 g / \left[(i\Delta + \kappa/2)^2 + g^2\right]\right|^2$, where $\Delta = \omega - \omega_{\rm in}$ ($\omega_{\rm in}$ is the frequency of the input laser), and g describes the coupling strength between the CW and CCW modes.

The expression of the reflection rate R is very simple and we can easily note two points with respect to an observable output beam intensity of the CCW modes. Firstly, to obtain a remarkable modal-coupling effect, the whole cavity decay κ cannot be too small compared with the coupling strength g. For instance, $R_{\rm max} \approx 0.25, 0.036$ for $g/\kappa = 1, 0.1$ respectively when $\kappa_1/\kappa_0 = 1$. Secondly, a relatively large κ_1/κ_0 is needed to ensure that the external losses dominate the total cavity dissipation, thus leading to an obvious directional emission. For example, $R_{\rm max}$ increases from 0.008 to 0.25 with κ_1/κ_0 from 0.1 to 1 when $g/\kappa = 1$.

In conclusion, through free-space modal coupling to a slightly deformed microsphere, we directly measured the lateral intensity distributions of WG modes. This experiment shows that modal coupling which results from the scattering formalism of traveling waves can play a significant role in a number of applications.

Y. Xiao gratefully thank Professor Kerry J. Vahala at Caltech for his numerous amendments and valuable suggestions to the current paper. C. Dong and Y. Xiao contribute equally to this paper. This work was supported by the National Fundamental Research Program of China (No. 2006CB921900), the Knowledge Innovation Project of Chinese Academy of Sciences, and the National Natural Science Foundation of China (No. 60537020 and 60621064). C. Dong's e-mail address is Dfrank.dch@gmail.com.

References

1. A. B. Matsko and V. S. Ilchenko, IEEE J. Sel. Top. Quantum Electron. **12,** 3 (2006).
2. K. J. Vahala, *Optical Microcavities* (World Scientific, Singapore, 2004).
3. R. K. Chang and A. J. Campillo, *Optical Processes in Microcavities* (World Scientific, Singapore, 1996).
4. J. R. Buck and H. J. Kimble, Phys. Rev. A **67,** 033806 (2003).
5. S. M. Spillane, T. J. Kippenberg, and K. J. Vahala, Phys. Rev. A **71,** 013817 (2005).
6. T. Aoki, B. Dayan, E. Wilcut, W. P. Bowen, A. S. Parkins, K. J. Vahala, T. J. Kippenberg, and H. J. Kimble, Nature **443,** 671 (2006).
7. P. E. Barclay, K. Srinivasan, and O. Painter, Appl. Phys. Lett. **89,** 131108 (2006).
8. T. A. Brun and H. Wang, Phys. Rev. A **61,** 032307 (2000).
9. W. Yao, R.-B. Liu, and L. J. Sham, Phys. Rev. Lett. **95,** 030504 (2005).
10. Y.-F. Xiao, Z.-F. Han, and G.-C. Guo, Phys. Rev. A **73,** 052324 (2006).
11. Y.-F. Xiao, X.-M. Lin, J. Gao, Y. Yang, Z.-F. Han, and G.-C. Guo, Phys. Rev. A **70,** 042314 (2004).
12. S. Götzinger, S. Demmerer, O. Benson, and V. Sandoghdar, Journal of Microscopy **202,** 117 (2001).
13. J. C. Knight, N. Dubreuil, V. Sandoghdar, J. Hare, V. Lefèvre-Seguin, J. M. Raimond, and S. Haroche, Opt. Lett. **20,** 1515 (1995).
14. L. Yang and K. J. Vahala, Opt. Lett. **28,** 080592 (2003).
15. V. S. Ilćhenko and M. L. Gorodetsky, Laser Phys. **2,** 1004 (1992).
16. T. J. Kippenberg, S. M. Spillane, and K. J. Vahala, Opt. Lett. **27,** 1669 (2002).
17. J. U. Nöckel and A. D. Stone, Nature **358,** 45 (1997).
18. M. L. Gorodetsky, A. D. Pryamikov, and V. S. Ilchenko, J. Opt. Soc. Am. B **17,** 1051 (2000).
19. M. Cai, O. Painter, and K. J. Vahala, Phys. Rev. Lett. **85,** 74 (2000).
20. C. Gmachl, F. Capasso, E. E. Narimanov, J. U. Nöckel, A. D. Stone, J. Faist, D. L. Sivco, and A. Y. Cho, Science **280,** 1556 (1998).
21. M. S. Kurdoglyan, S.-Y. Lee, S. Rim, and C.-M. Kim, Opt. Lett. **29,** 2758 (2004)
22. M. Kneissl, M. Teepe, N. Miyashita, and N. M. Johnson, Appl. Phys. Lett. **84,** 2485 (2004).
23. T. Ben-Messaoud and J. Zyss, Appl. Phys. Lett. **86,** 241110 (2005).
24. S. Lacey, H. Wang, D. H. Foster, and J. U. Nöckel, Phys. Rev. Lett. **91,** 033902 (2003).
25. Y.-S. Park, A. K. Cook, and H. Wang, Nano Lett. **6,** 2075 (2006).
26. V. B. Braginsky, M. L. Gorodetsky, and V. S. Ilchenko, Phys. Lett. A **137,** 393 (1989).
27. J.-M. Le Floch, J. D. Anstie, M. E. Tobar, J. G. Hartnett, P.-Y. Bourgeois, and D. Cros, Phys. Lett A **359,** 1 (2006).
28. W. Li and R. Wang, Chin. Opt. Lett. **2,** 271 (2004).